Dynamic Mechanical Properties of Highly Loaded Ferrite-Filled Thermoplastic Elastomer*

D. R. SAINI, A. V. SHENOY, and V. M. NADKARNI, *Polymer Science and Engineering Group, Chemical Engineering Division, National Chemical Laboratory, Pune 411 008, India*

Synopsis

The dynamic mechanical properties in terms of the storage modulus E', loss modulus E'', and the loss tangent δ has been studied for highly filled magnetic polymer composites. The effect of surface treatment on the relaxation spectra has been clearly elucidated and quantitative values indicating the extent of polymer–filler interactions have been given. Various models have been tested for describing the viscoelastic behavior of such highly filled systems. The Wiechert model using a single-arm with a Cole–Cole parameter has been shown to effectively fit the Argand diagram in the case of the present highly filled systems.

INTRODUCTION

Magnetic polymer composites have gained considerable commercial importance[1-7] due to their wide applications in clamps, refrigerator door latches, bearing sleeves, timing-motor rotors, etc. Compared to ceramic magnets, the magnetic polymer composites offer a greater degree of design flexibility and improved processibility. These composite materials are fabricated by incorporating over 60–70% by volume or, in other words, 87–92% by weight of barium or stronium ferrites in appropriate polymeric matrices. Such high loadings are a must in order to achieve the desired magnetic strengths comparable to ceramic magnets. The polymeric materials only act as binders to provide the design and processing economics of plastics to the rigid filler particles. The choice of the matrix governs whether the final product would form a flexible or a molded magnet. Such high loadings of the ferrites make the retention of the matrix flexibility quite a challenging task. Moreover, at loadings over 50% by volume, strong particle–particle interactions of the network type would result in poor dispersion, reduced processibility, and itself provide a difficult task to look for means of maintaining the process economics.

Despite the challenges extended in the manufacture of magnetic polymer composites, there have been no fundamental studies on such systems in the literature besides the recent attempts by Saini et al.[8-11] The steady-state melt viscosity behavior,[8] the dynamic rheological characteristics of the melts,[9] the effect of surface treatment on the rheological, mechanical, and magnetic properties[10] as well as the mechanical properties of the magnetic polymer composites[11] have all been comprehensively studied by Saini et al. Most of the other literature on magnetic polymer composites such as se-

* NCL Communication No. 3407.

Journal of Applied Polymer Science, Vol. 29, 4123–4143 (1984)
 CCC 0021-8995/84/124123-21$04.00

lection of the matrix materials that offer flexibility even at such high levels of ferrite loadings is in the form of patents.[5]

In the present article, the dynamic mechanical properties of the magnetic polymer composites have been studied. Such a study is useful in adjudging the behavior of the composites in their end-product applications. In most of the applications, the magnetic polymer composites would be subjected to vibrations or loads which vary with time. Dynamic mechanical data would provide an insight into the response of the material to forced oscillation, its capacity to damp vibration and also provide a measure of the impact strength of the material. A knowledge of these properties would, undoubtedly, be useful when considering applications such as refrigerator door latches, timing-motor rotors, and bearing sleeves.

BACKGROUND

Dynamic mechanical testing is a powerful tool for obtaining valuable structural and morphological information of unfilled and filled systems when they are subjected to dynamic load over a broad range of temperature and frequency. There are a number of investigators[12-24] who have studied the dynamic behavior of filled polymers and have concluded that the mechanical behavior of composites under dynamic conditions is dependent on the nature of the polymer matrix, the filler size, shape, and size distribution as well as the nature of the polymer–filler interface, namely, on the type and amount of surface modifier. Surface treatment of fillers to improve polymer–filler interaction has been popular recently, and there are number of publications in the recent past dealing with their effect on rheological and mechanical properties.[24-40] Despite the obvious relevance of dynamic measurements for magnetic polymer composites, there have been no studies in the past on the structural and morphological evaluation of such systems. The present paper deals with the study of the effect of very high loading of ferrites and the effect of type as well as amount of surface treating agents on the dynamic mechanical properties of barium ferrite styrene–isoprene–styrene composites.

EXPERIMENTAL

Materials

Filler. Barium ferrite of chemical composition $BaFe_{12}0_{19}$ supplied specifically for this study by Morris-Electronics, Pune, India is used as the filler. The specific gravity of the filler is 4.0, the average particle size about 3 μm and the shape of the filler being platelet in form.

Matrix. The matrix used is styrene–isoprene–styrene Kraton 1107 supplied to us by Shell Chemie, Switzerland.

Surface-Treating Agents. The surface modifiers used were those taken from the broad category of silanes and titanates; the details of these are given in Table I. The silane was supplied to us free of charge by Dow Chemicals, and the titanate was made available by Kenrich Petrochemicals free of charge through their agents in India (TWILL, Bombay).

TABLE I
Summary of the Surface Modifiers Investigated

Trade codes	Chemical description	Chemical structure
Z-6076	Chloropropyltrimethoxy silane	$Cl(CH_2)_3Si(OCH_3)_2$
KR-TTS	Isopropyl triisotearoyl titanate	$CH_3-\underset{\displaystyle CH_3}{\underset{\vert}{CH}}-O-Ti-[O-\overset{\displaystyle O}{\overset{\Vert}{C}}-C_{17}H_{35}]_3$

Sample Preparation

Surface Treatment. The required quantity of barium ferrite was taken in a flask, and the surface modifiers were added to the solution to form a slurry. For the silane, a solution in 95% methanol and 5% water by volume was prepared while, for the titanate, a solution using xylene was prepared. One percent by weight of barium ferrite of the surface modifier was added to slurry and stirred with a glass rod for 30 min. After an overnight stand, the solvent was removed by heating in an oven at 105°C for silane and 130°C for titanate.

Compounding. Experimental compositions of 75%, 80%, and 85% by weight of untreated ferrites as well as 85% by weight each of the treated ferrites with required quantity of SIS Kraton 1107 were prepared using a 70 cc roller-type mixing chamber of a C.W. Brabender PLE 330. The blending was done at a rotational speed of 125 rpm at the temperature of 180°C till the recorded torque reached an equilibrium value, which in all cases took an approximate duration of about 3 min.

Test Specimens. Sheets of the thickness of 0.028 cm were prepared on the roll mill using the compounded materials. The required sized test specimens 2.1 × 0.5 cm were cut from the sheets by careful use of a sharp cutting tool.

Testing Method

Dynamic Mechanical Measurements. The dynamic mechanical properties in terms of storage modulus E', loss modulus E'', and damping factor tan δ for each of the composites under investigation was studied using the Rheovibron Viscoelastometer DDV-II-C (Toyo Baldwin Co. Ltd.) over a range of temperature at 11 Hz. An extensive treatment of dynamic mechanical testing and viscoelasticity can be found in the literature[41-51] and can be referred to for details.

RESULTS AND DISCUSSION

Figures 1–6 show the variation of the storage modulus E' and the loss tangent δ with temperature. The loss peaks that are observed in each graph correspond to α-transition, namely, the lower glass transition of the system. It must be noted that the polymeric matrix SIS has two distinct glass transition temperatures corresponding to each block in the polymer chain[52] for the high molecular weight SIS. The lower glass transition temperature T_g corresponds to a temperature of about −48°C from the α-peak temper-

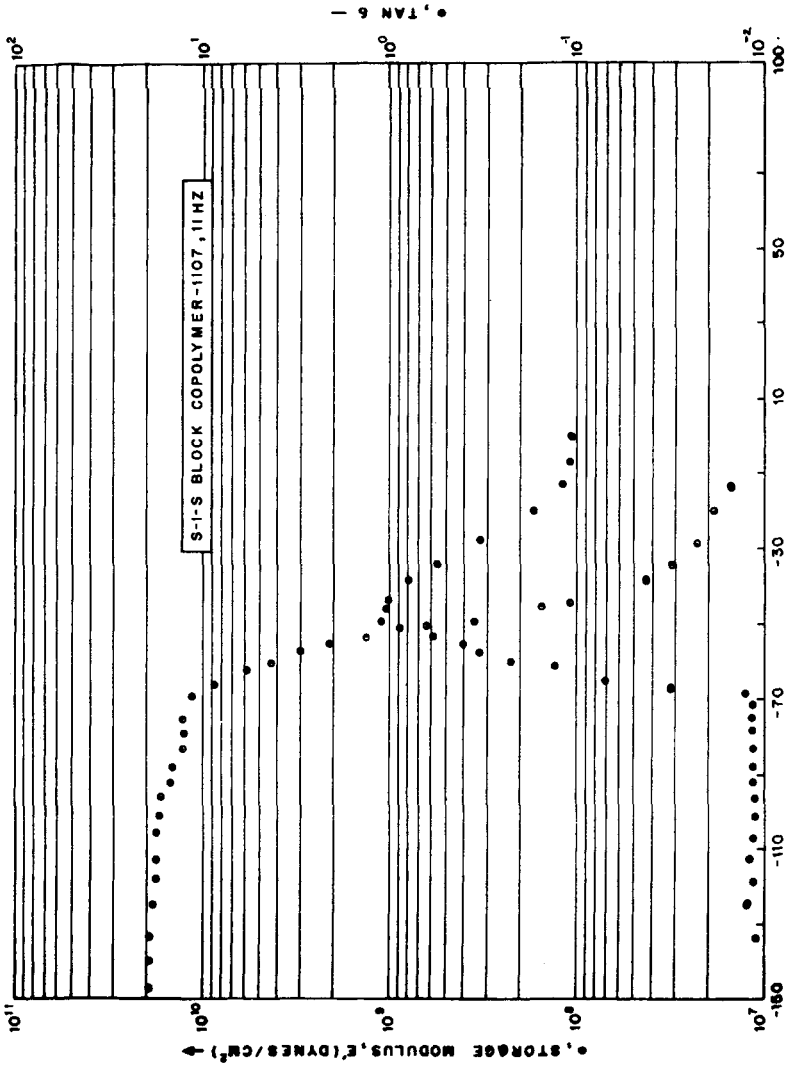

Fig. 1. Variation of E' and tan δ with temperature for unfilled S-I-S.

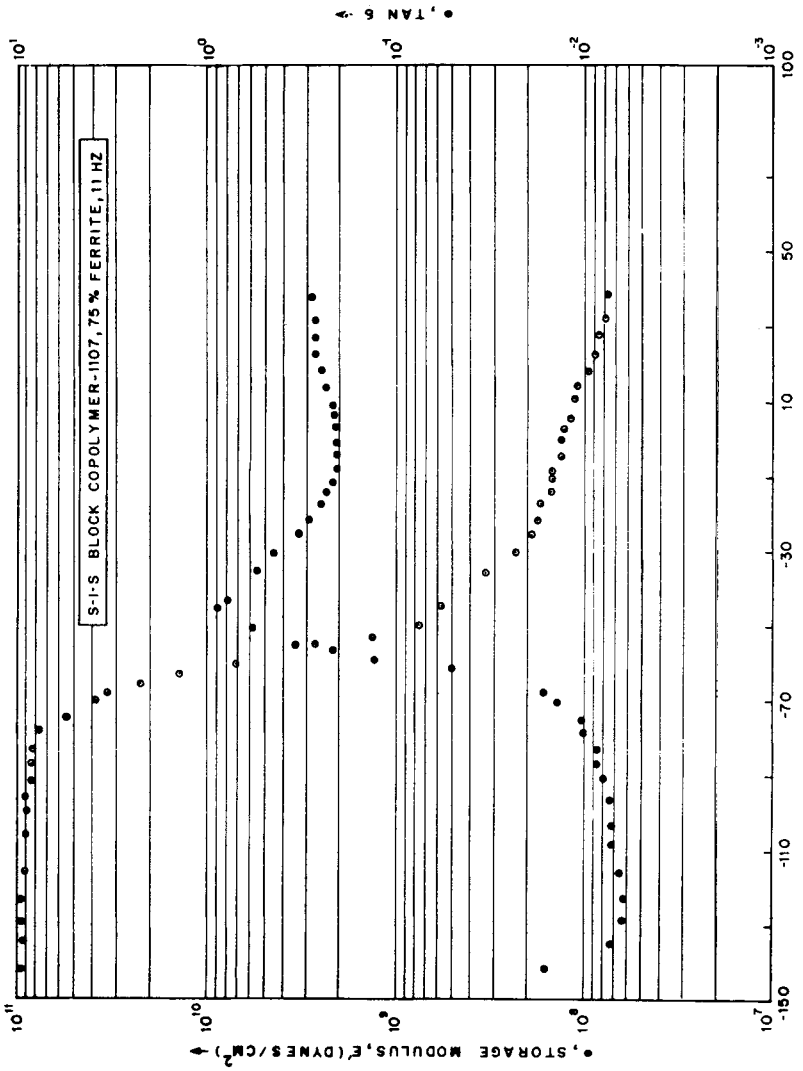

Fig. 2. Variation of E' and tan δ with temperature for SIS with 75 wt % ferrites.

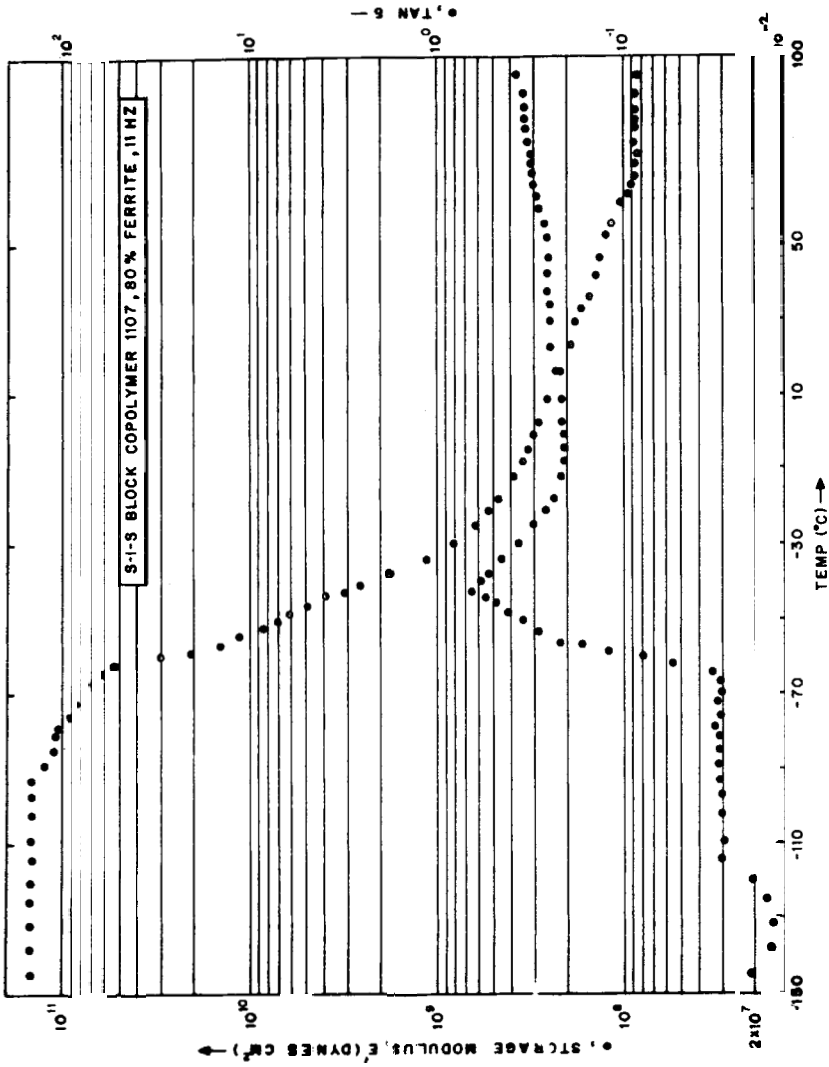

Fig. 3. Variation of E' and tan δ with temperature for SIS with 80 wt % ferrites.

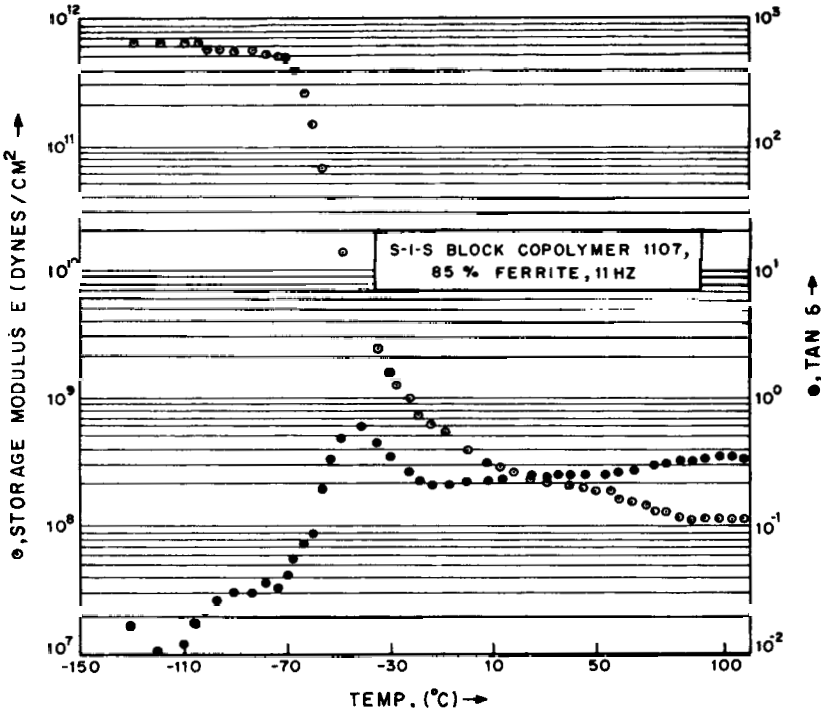

Fig. 4. Variation of E' and tan δ with temperature for SIS with 85 wt % ferrites.

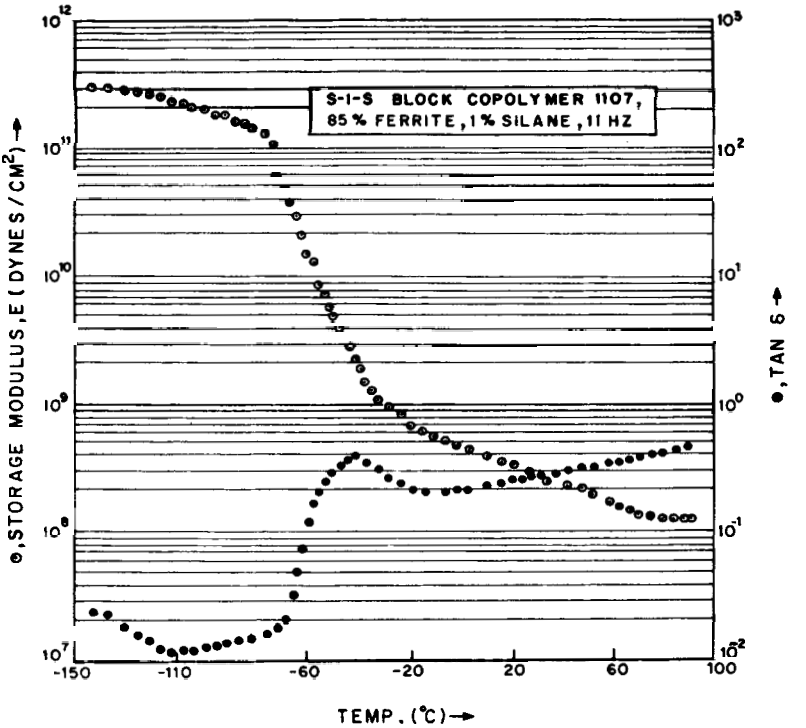

Fig. 5. Variation of E' and tan δ with temperature for SIS with 85 wt % ferrite surface treated with Z-6076.

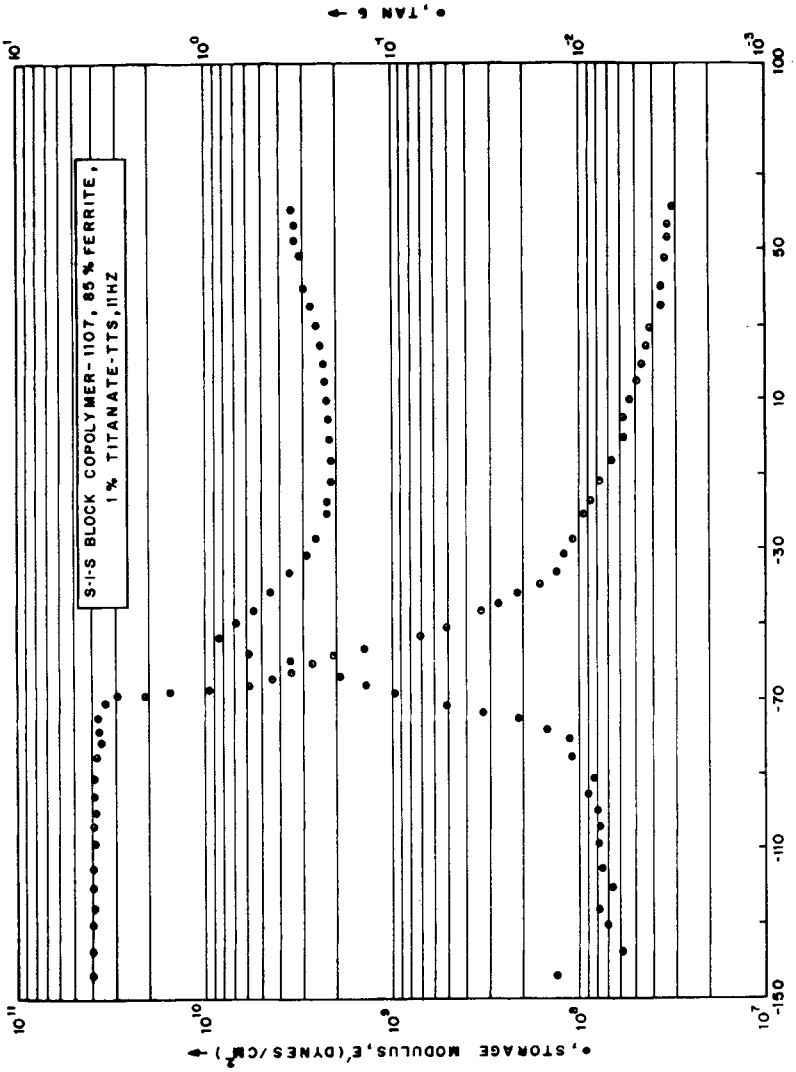

Fig. 6. Variation of E' and tan δ with temperature for SIS with 85 wt % ferrite surface treated with KR-TTS.

ature in Figure 1. This can be seen to fall within the range determined by Widmaier and Meyer[53] for a number of SIS samples of different molecular weights. The other dispersion peaks were not detectable at the frequency of working. At the α-transition, the greatest decrease in the dynamic modulus is also seen with increasing temperature. The profound effects on tan δ and dynamic modulus are seen at the α-transition because this change corresponds to the molecular micro-Brownian motions of long chain segments in the polymer structure rather than motions in the side groups as in the case of β-transition or the γ-transition. The glass transition phenomena which occurs at the α-transition affects the peak height, the temperature of the α peak and the onset of the transition. These important parameters as well as others corresponding to the storage modulus have been given in Table II.

It is seen that the addition of the filler increases the glass transition temperature in accordance with all earlier findings,[53-59] which report increases in T_g as a function of filler content for composites involving a wide variety of polymers and a number of different fillers. The increases in T_g have been postulated to be a result of the polymer–filler interaction due to the interfacial forces between the filler and chain, orientation of the chain in the immediate vicinity of the filler surface, the formation of an interface or any other physicochemical phenomena. Ziegel and Romanov[60] have suggested the evaluation a parameter B which presents the extent of the polymer–filler interaction by comparing the loss moduli E'' of the filled and unfilled systems as

$$\frac{E''_c}{E''_p} = [1 - (\phi_f B)^n]^{-1} \tag{1}$$

where E''_p and E''_c are the loss moduli of the unfilled and filled systems, respectively. A plot of the logarithm of $1 - E''_p/E''_c$ vs. the logarithm of ϕ_f must yield a straight line from which the exponent n can be evaluated as the slope and the parameter B from the intercept. In the present case, this plot has been shown in Figure 7, and the values of the respective parameters as calculated from the figure are $n = 1.4$ and $B = 1.56$. Using eq. (1), it is thus possible to predict E''_c at even higher loadings such as 90% by weight, which are of true pragmatic importance.

The parameter B is related with the geometry of the filler particle and the effective thickness R of the interfacial region for the case of a platelet shaped particle as follows[61]:

$$B = (1 + 2\Delta R/D)^2 (1 + 2\Delta R/x) \tag{2}$$

where D is the width of the platelet and x is its thickness. An increase in ΔR would suggest strong interaction. Thus larger the value of B the greater is the interaction.

Surface treatment can be seen to have an effect on the T_g in relation to the type of surface treatment. It is found that silane does not affect the T_g of the 85 wt % filled system while titanate drastically lowers it. There is evidence in the literature that fillers with different surface properties[62] increase the T_g in relation to the polymer–filler interaction energy while

TABLE II
Test Data Summary[a]

Matrix	Filler amount by wt %	Type of surface-treating agent	Storage modulus data: T (°C) On set	T (°C) E' (3×10^9)	T (°C) E'(R)	E'(10^8 dyn/cm^2) Onset	E'(10^8 dyn/cm^2) E'(R)	Loss tangent data: T (°C) α-Peak onset	T (°C) α-Peak max	T (°C) Tan δ = 0.2	$W_{0.2,c}$
SIS	—	—	−70.0	−57.0	−30.0	120.0	0.2	−7.0	−48.0	−60.0	3.8
SIS	75	—	−78.0	−55.0	−25.0	800.0	1.9	−8.0	−45.0	−59.0	5.2
SIS	80	—	−90.0	−43.0	−10.0	1000.0	3.6	−9.0	−43.0	−57.0	4.7
SIS	85	—	−67.0	−37.0	0.	4000.0	4.0	−14.0	−41.0	−56.0	4.3
SIS	85	Z-6076	−70.0	−44.0	0.	5000.0	4.5	−14.0	−40.0	−55.0	4.2
SIS	85	KR-TTS	−70.0	−62.0	−27.0	360.0	1.0	−10.0	−53.0	−63.0	5.8

[a] $W_{0.2}$ = peak width at tan δ = 0.2; E' (3×10^9) = storage modulus value is 3×10^9 dyn/cm^2; E'(R) = storage modulus value at onset of rubbery region.

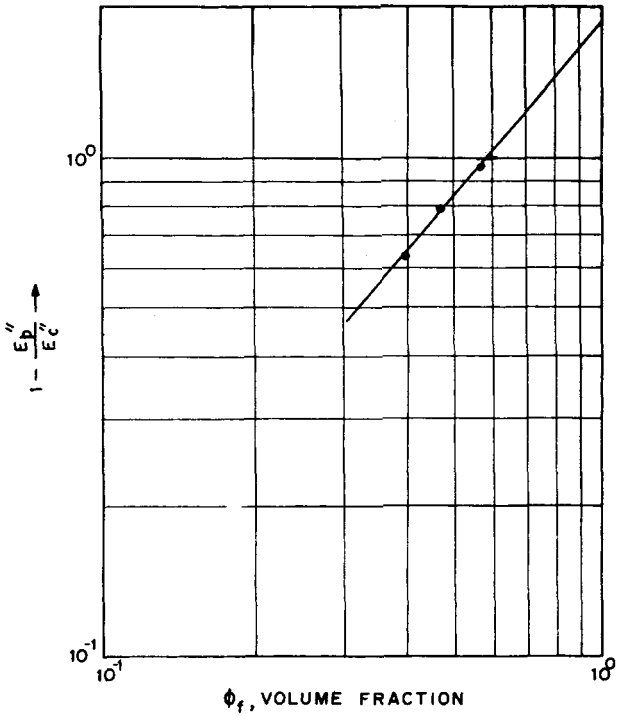

Fig. 7. Variation of $1 - E_p''/E_c''$ vs. ϕ_f at the loss modulus maxima.

the plasticizers are known to decrease the T_g.[63] Iisaka and Shibayama[64] have shown that, with increasing particle size, T_g increases in the case of mica-filled system. It is known that mica is a platelet in form and hence the effects on it should be similar to those observed in the case of ferrite-filled systems. Surface treatment that leads to coupling would depict a behavior similar to an apparent particle size increase. Coupling between the filler and matrix is likely to extend the thickness of the partially immobilized layer, resulting in an apparent increase in the specific surface area of the filler per gram of polymer. Iisaka and Shibayama have proposed an equation for T_g in order to relate its changes to particle size of filler. This equation as given below

$$T_g = K_f \ln S \tag{3}$$

where K_f is a constant and S is the specific surface area of the filler per gram of polymer, clearly suggests that, with greater polymer–filler interaction, the T_g would increase. Based on the same equation, the effect of a plasticizer could be explained on the basis that it reduces the partially immobilized layer leading to a decrease in the specific surface area of the filler per gram of polymer. Titanates act as plasticizer and decrease the polymer–filler interaction, thus leading to a decrease in the T_g.

The effect on polymer–filler interaction due to changes in the surface activity of the filler can be studied by the approach suggested by Lepie and Adicoff.[17] They related the peak height of tan δ to the differences in the

void concentrations ΔC between composites 1 and 2 by the following equation:

$$\ln \frac{\tan \delta_1}{\tan \delta_2} = -k\Delta C \tag{4}$$

where k is a constant.

From this equation, it can be deduced that the efficiency of surface-active agents in preventing void formation at the interface should be inversely related to the peaks of tan δ.[19] If tan δ_2 is taken as the peak height for 85 wt % ferrite-filled system and tan δ_1 as the peak height for different surface treatments, an immediate estimate of the void formation can be obtained from eq. (4). The values of ln (tan δ_1/tan δ_2) have been shown in Table III and indicates that surface treatment does have an effect on void formation and hence filler dispersion.

There are a number of expressions available in the literature for modelling the E' and tan δ values of composites based on the concentration of the filler. The various expressions have been summarized by Chacko et al.[24] They found that, at low concentrations of the dispersed phase, the Voigt model, the Dewey–Goodier model, and the Christensen–Lo-Kerner model all gave extremely close predictions. However, the discrepancies between the predicted and experimentally obtained values for both modulus and damping of polymer filler composites were quite severe at higher volume concentrations. Reasons for such deviations have been postulated[20,65] and methods of corrections suggested. In all cases, the maximum amount of filler used was not over 40% by weight corresponding to less than 25% by volume. In the present case, since the loading is of the order of 75–85% by weight, it would be worth investigating the nature of the failure of the proposed models for the dynamic mechanical measurements of composites.

TABLE III

A. Effect of Filler Amount on Polymer–Filler Interaction [eq. (4)]

Matrix	Filler amount by wt %	ln (tan δ_1/tan δ_2)
SIS	—	0
SIS	75	−0.173
SIS	80	−0.453
SIS	85	−0.578

B. Effect of Surface Treatment on Polymer–Filler Interaction [eq. (4)]

Matrix	Filler amount by wt %	Type of surface treating agent	ln (tan δ_1/δ_2)
SIS	85	—	0
SIS	85	Z-6076	−0.405
SIS	85	KR–TTS	+0.348

The Voigt model is the theoretical lower bound on the composite modulus while the Reuss model is the theoretical upper bound. The expressions for E'_c can be written for each of the two models as follows:

Voigt model:
$$\frac{E'_p}{E'_c} = (1 - \phi_f) + \phi_f \frac{E'_p}{E'_f} \tag{5}$$

Reuss model:
$$\frac{E'_c}{E'_p} = (1 - \phi_f) + \phi_f \frac{E'_f}{E'_p} \tag{6}$$

where ϕ_f is the filler volume concentration and subscripts c, f, and p refer to composite, filler, and polymer, respectively. Equations (5) and (6) suggest that a straight line plot of E'_p/E'_c vs. ϕ_f or E'_c/E'_p vs. ϕ_f would indicate a good model fit. Figure 8 shows the plots of E'_p/E'_c vs. ϕ_f for the Voigt model in three different cases of temperature. Each of the curves basically represent the variation of E'_p/E'_f, namely, the slope of the plots. It is seen that the curves are nonlinear at such high levels of loading, thus suggesting that the particle–particle and particle–polymer interactions play a dominating role in shifting the composites from their model predictions.

A phenomenological model of the Wiechert spring–dashpot array type[51] may be tested for providing a reasonable prediction of the elastic and loss modulus of the composites at arbitrary temperatures and driving frequencies.

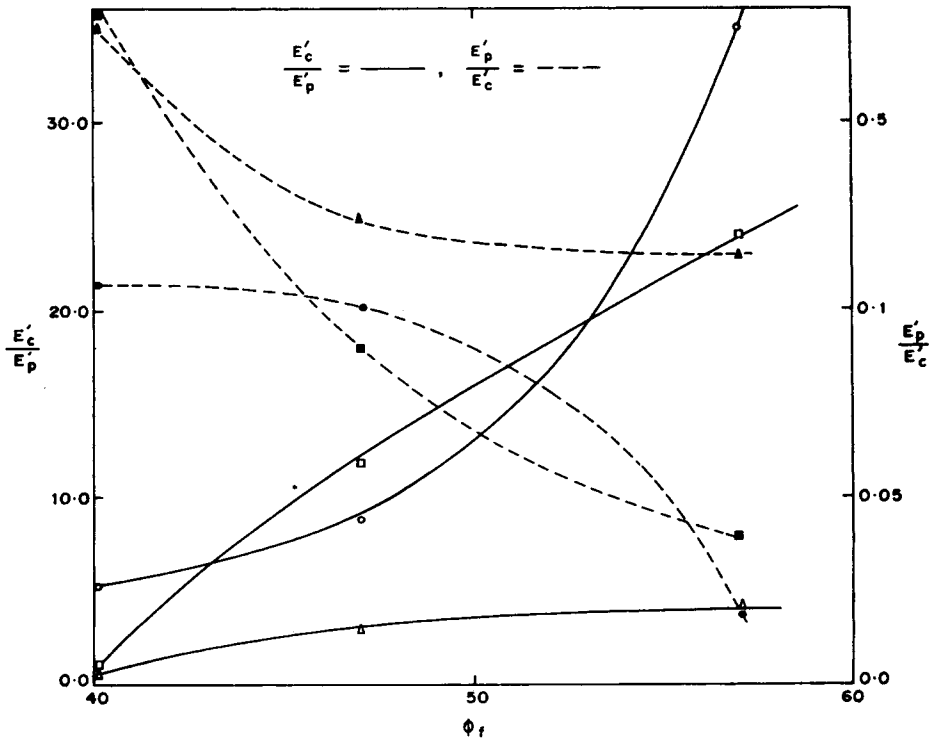

Fig. 8. Variation of E'_p/E'_c vs. ϕ_f at various temperatures.

The complex modulus E^* in the jth arm of the Wiechert model can be written as

$$E^* = k_e + \sum_{j=1}^{n} \frac{k_j(iw)}{1 + iw\tau_j} \tag{7}$$

where k_e is the equilibrium spring constant, k_j is the spring constant in the jth arm, τ_j is the relaxation time in the jth arm, and w is the frequency. The storage (real) and the loss (imaginary) components of the complex modulus can be written explicitly from the above equation as follows:

$$E' = k_e + \sum_{j=1}^{n} \frac{k_j w^2 \tau_j^2}{1 + w^2\tau_j^2} \tag{8}$$

$$E'' = \sum_{j=1}^{n} \frac{\bar{k}_j w\tau_j}{1 + w^2\tau_j^2} \tag{9}$$

In the above Wiechert model, the general practice is to use one arm for each observed transition and assign a single relaxation time to each transition. Single relaxation time model, theoretically, would not provide a complete description of the experimental data, since the molecular mechanisms involved even in a single transition are sufficiently dissimilar to create a wide distribution of relaxation times. One means of improving the model is to assign several Wiechert arms to each transition. Another approach is to modify eq. (7) slightly to include a Cole–Cole broadening parameter β_j on each arm:

$$E^* = k_g - \sum_{j=1}^{n} \frac{k_j}{1 + (iw\tau_j)\,\beta_j} \tag{10}$$

where $k_g = k_e + \Sigma k_j$. A convenient means of selecting the parameters for the Wiechert model is to employ the Argand diagram in which E'' is plotted as the ordinate against E' as the abscissa. In the case of single-relaxation time transitions, this diagram appears as a semicircle which intersects the abscissa at the maximum and minimum storage moduli. In the case of the distributed relaxation times, the semicircles are depressed to arcs, and it can be shown that the height of the arc is directly related to the Cole–Cole broadening parameter as

$$\beta = \frac{4}{\pi} \tan^{-1} \frac{2E''_{\max}}{E''_{\max} - E'_{\min}} \tag{11}$$

The equilibrium spring constant k_e in the Wiechert model is taken as equal to $E'_{\min}$ while k_j is set equal to $E'_{\max} - E'_{\min}$ and $\bar{k}_j$ is set equal to $2E''_{\max}$. Figures 9–14 show plots of Argand diagrams in the present case. The points represent experimental values while the solid line gives the single-arm model fit. The values of the model parameter are tabulated in Table IV. The model predictions required the estimation of the relaxation time τ. For

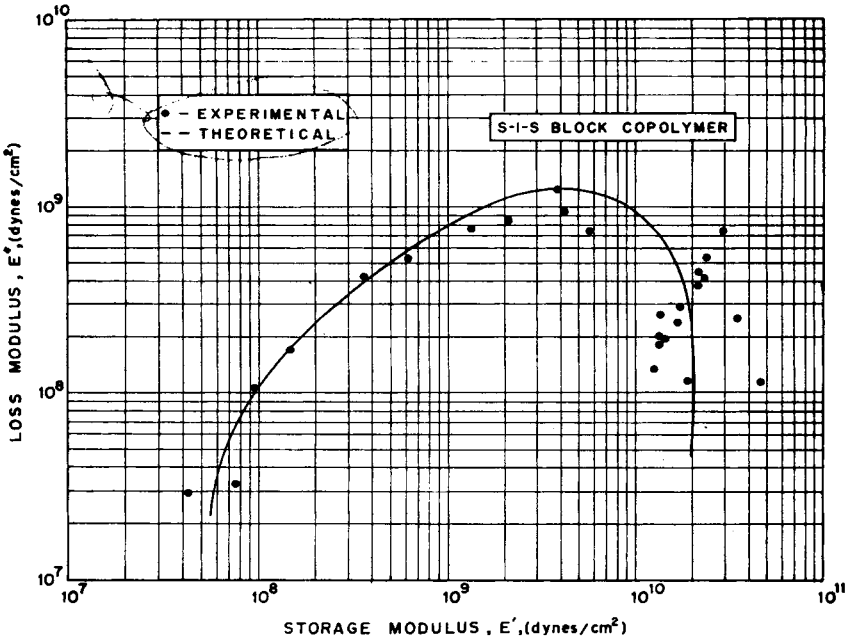

Fig. 9. Argand diagram for SIS: (●) experimental; (——) theoretical.

a reasonable temperature dependence for the model, the relaxation time is assumed to follow the Eyring's equation

$$\tau = \tau_0 \exp(H/RT) \tag{12}$$

where τ_0 is a preexponential time, H is an apparent activation energy of the process, T is the absolute temperature, and $R = 8.314$ J/mol · K is the gas constant. The numerical value of τ_0 may be obtained by noting that $\omega\tau = 1$ at the center of the transition, where E'' passes through a maximum on the E'' vs. T plot. Thus

$$\tau_0 = (1/\omega) \exp(H/RT_0) \tag{13}$$

where T_0 is the temperature at the transition midpoint.

TABLE IV
Numerical Parameters for the Wiechert Model

Matrix	Filler amount by wt %	Type of surface treating agent	k_e	k_1	$\bar{k}_1$	β	H
SIS	0	—	3.0×10^7	1.9×10^{10}	2.5×10^9	9.23	4.96×10^4
SIS	75	—	7.0×10^7	9.5×10^{10}	4.0×10^9	3.80	2.38×10^4
SIS	80	—	9.3×10^7	1.2×10^{11}	6.0×10^9	3.44	2.18×10^4
SIS	85	—	2.0×10^8	5.9×10^{11}	2.6×10^{10}	3.04	1.98×10^4
SIS	85	Z-6076	1.8×10^8	2.9×10^{11}	4.2×10^9	1.05	1.58×10^4
SIS	85	KR-TTS	3.2×10^7	3.9×10^{10}	2.6×10^9	4.30	1.39×10^4

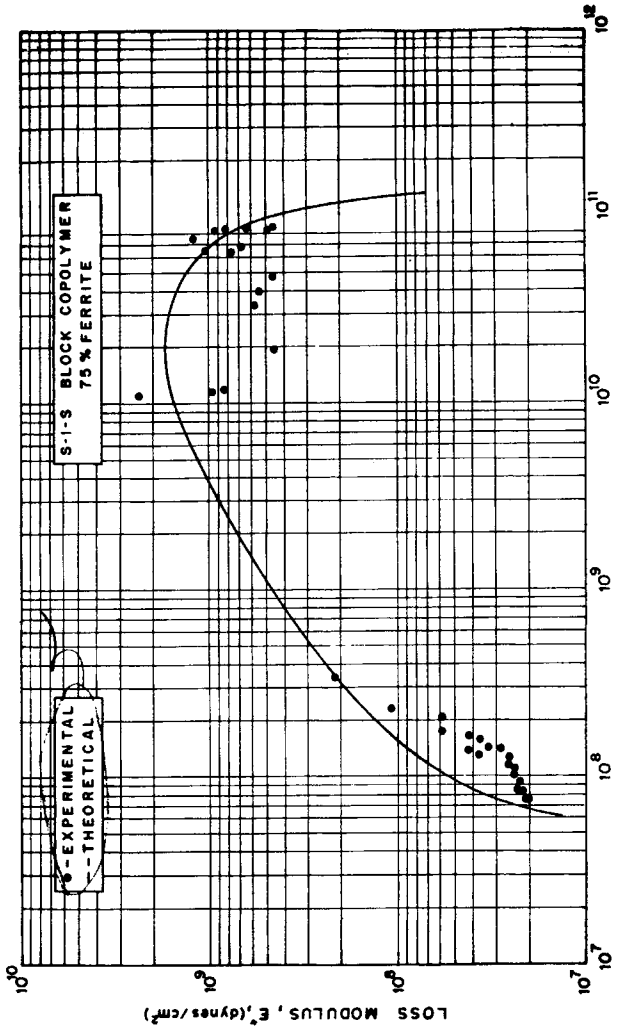

Fig. 10. Argand diagram for SIS with 75 wt % ferrites: (●) experimental; (——) theoretical.

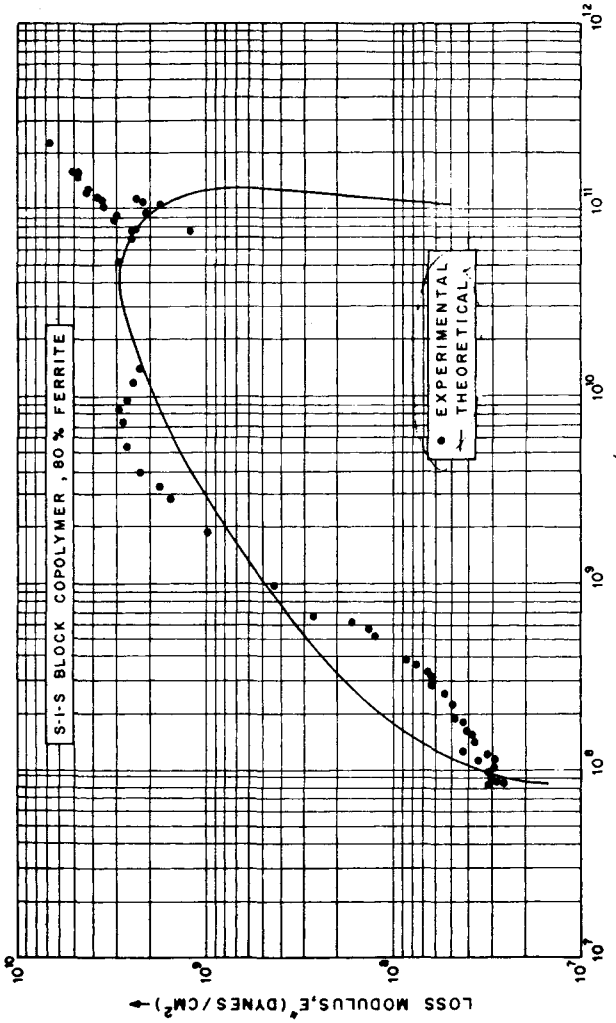

Fig. 11. Argand diagram for SIS with 80 wt % ferrites: (●) experimental; (——) theoretical.

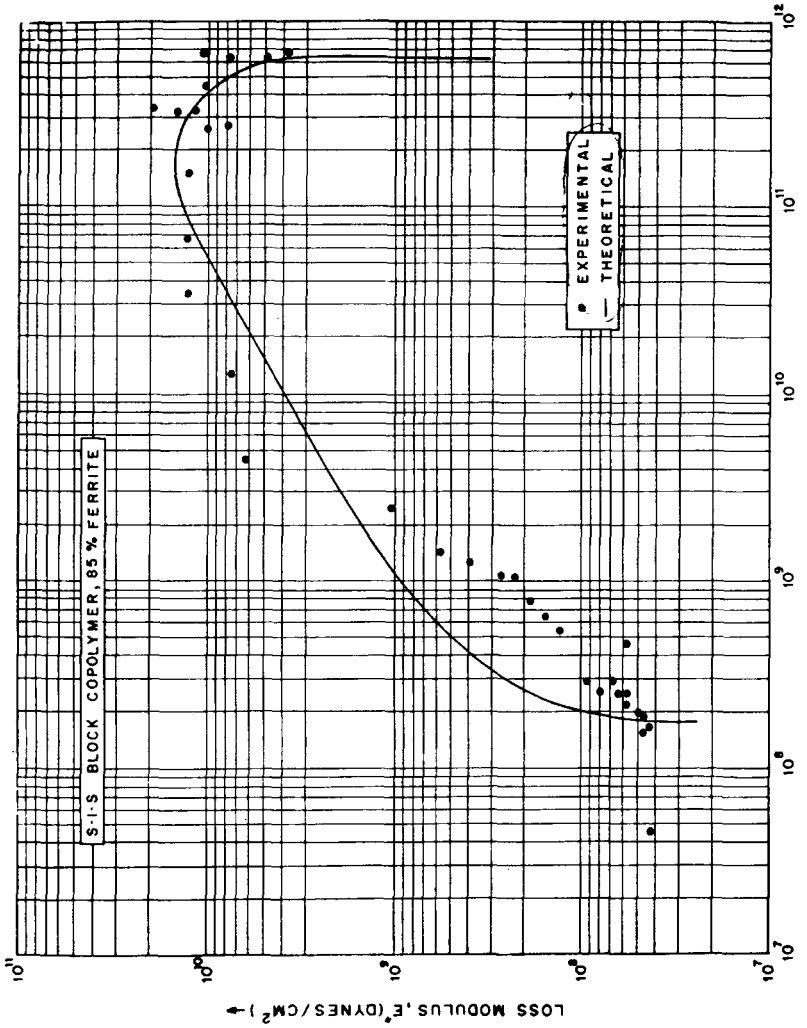

Fig. 12. Argand diagram for SIS with 85 wt % ferrites: (●) experimental; (——) theoretical.

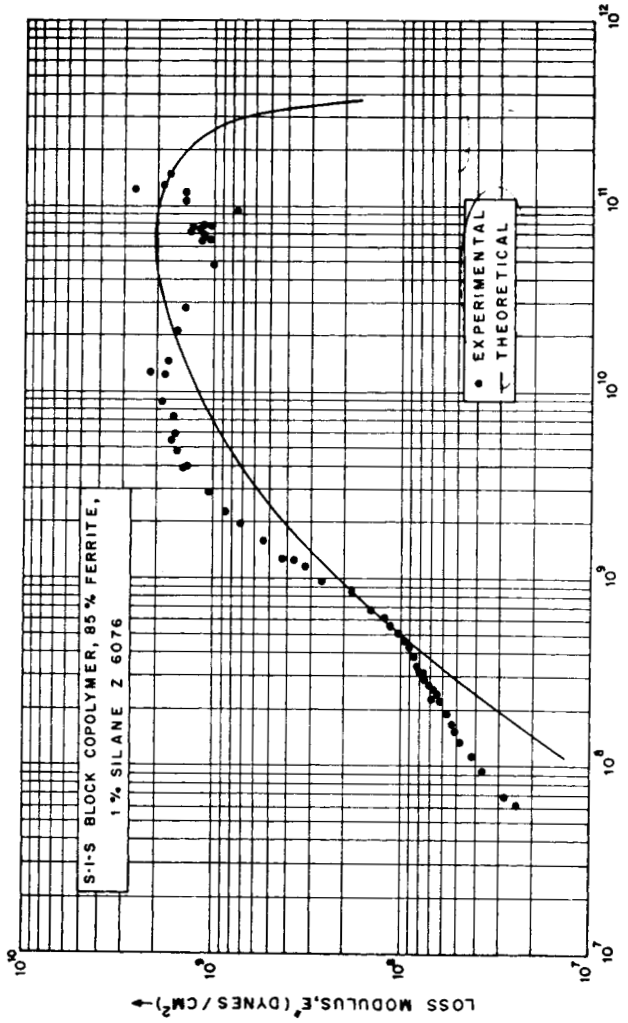

Fig. 13. Argand diagram for SIS with 85 wt % ferrites surface treated with Z-6076: (●) experimental; (——) theoretical.

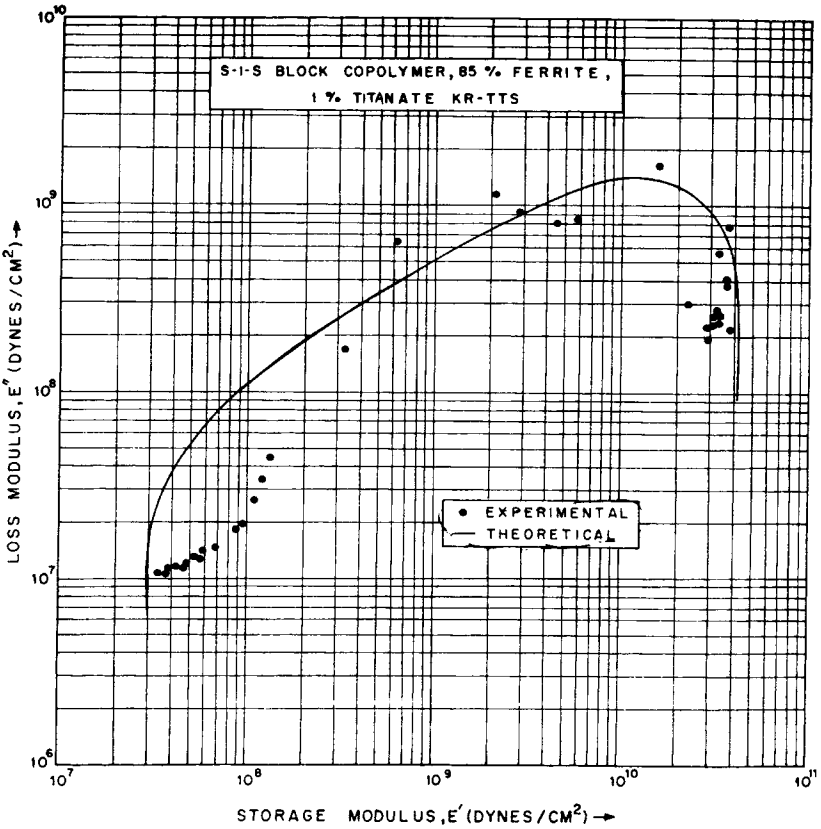

Fig. 14. Argand diagram for SIS with 85 wt % ferrites surface treated with KR-TTS: (●) experimental; (——) theoretical.

The value of the activation energy can be obtained conveniently[51] from the inverse value of the area under the plot of E'' vs. $1/T$. The values of the estimated activation energies are also given in Table IV. The solid lines in Figures 9–14 show the reasonably good theoretical predictions of the Wiechert model.

References

1. M. Janu and O. Kubicek, *Int. Chem. Eng.*, **2**, 526 (1962).
2. J. Theberge, B. Arkles, and D. Knabb, *Machine Design*, 3 (Feb. 1977).
3. K. Mizuno, M. Takata, and H. Yanagida, **57**, 519 (1978).
4. Z. E. Kerekes, in *Handbook of Fillers and Reinforcements for Plastics*, H. S. Katz and J. V. Milewski, Eds., Van Nostrand Reinhold, New York, 1978, Chap. 12, p. 205.
5. Y. Fukuyama, S. Habu, and T. Hayashi, *Int. Polym. Sci. Tech.*, **6**, T/78 (1979).
6. *Plastics Design Forum*, 70 (Jan./Feb. 1981).
7. J. E. Therberge, *Polym. Plast. Technol. Eng.*, **16**, 4 (1981).
8. D. R. Saini, A. V. Shenoy, and V. M. Nadkarni, *Polym Eng. Sci.*, to appear.
9. D. R. Saini and A. V. Shenoy, *Polym. Eng. Sci.*, to appear.
10. D. R. Saini, A. V. Shenoy, and V. M. Nadkarni, *Polym. Eng. Sci.*, to appear.
11. D. R. Saini, V. M. Nadkarni, K. D. P. Nigan and P. D. Grover, *J. Comp. Matl.*, to appear.
12. R. D. Bohme, *J. Appl. Polym. Sci.*, **12**, 1097 (1968).
13. L. E. Nielsen, *Trans. Soc. Rheol.*, **13**, 141 (1969).
14. T. B. Lewis and L. E. Nielsen, *J. Appl. Polym. Sci.*, **B14**, 1449 (1970).
15. J. L. Kardos, W. L. McDonnell, and J. Raisoni, *J. Macromol. Sci.*, **B6**, 397 (1972).
16. T. Hirai and D. E. Kline, *J. Compos. Mater.*, **7**, 160 (1973).
17. A. H. Lepie and A. Adicoff, *J. Appl. Polym. Sci.*, **16**, 1155 (1972).

18. A. H. Lepie and A. Adicoff, *J. Appl. Polym. Sci.*, **18**, 2165 (1974).
19. G. Perrault and G. Duchesne, *J. Appl. Polym. Sci.*, **18**, 1295 (1974).
20. B. L. Lee and L. E. Nielsen, *J. Polym. Sci.*, **B15**, 683 (1977).
21. L. F. Bryne and D. J. Hourston, *J. Appl. Polym. Sci.*, **23**, 2899 (1979).
22. S. A. Paipetis and P. Grootenhuis, *Fibre Sci. Technol.*, 353 (1979).
23. S. A. Paipetis and P. Grootenhuis, *Fibre Sci. Technol.*, 377 (1979).
24. V. P. Chacko, F. E. Karasz, and R. J. Farris, *Polym. Eng. Sci.*, **22**, 968 (1982).
25. E. P. Plueddemann, in *Interfaces in Polymer Matrix Composites*, E. P. Plueddemann, Ed. Academic, New York, 1974, Chap. 6.
26. S. J. Monte, *Mod. Plast. Encycl.*, **54**, 168 (1977).
27. M. S. Boira and C. E. Chaffey, *Polym. Eng. Sci.*, **17**, 715 (1977).
28. J. B. Marsden, *Plastic Compounding*, **1**, 32 (1978).
29. J. R. Copeland and O. W. Rush, *Plastic Compounding*, (Nov./Dec. 1978).
30. C. D. Han, C. Sandford, and H. J. Yoo, *Polym. Eng. Sci.*, **18**, 849 (1978).
31. S. J. Monte and G. Sugerman, *Polym. Plast. Technol. Eng.*, **13**, 115 (1979).
32. A. A. Schoenogood, *Plast. Eng.*, **35**, 25 (1979).
33. D. E. Cope and E. Linnert, *Plast. Eng.*, 37 (June 1980).
34. M. Hancock, P. Tremayne, and J. Rosevear, *J. Polym. Sci., Polym. Chem. Ed.*, **18** 3211 (1980).
35. C. D. Han, T. Van den Weghe, P. Shete, and J. R. Haw, *Polym. Eng. Sci.*, **21**, 198 (1981).
36. S. H. Morrell, *Plast. Rubber Proc. Appl.*, **1**, 179 (1981).
37. T. Nakatsuka, H. Kawasaki, K. Itadani, and S. Yamashita, *J. Appl. Polym. Sci.*, **27**, 259 (1982).
38. A. Garton, S. W. Kim, and D. M. Wiles, *J. Appl. Polym. Sci.*, **27**, 4179 (1982).
39. V. P. Juskey and C. E. Chaffey, *Can. J. Chem. Eng.*, **60**, 334 (1982).
40. D. M. Bigg, Polym. Eng. Sci., **22**, 512 (1982).
41. M. Takayanagi, Men. Fac. Eng., Kyushu Univ., **23** (1), (1963).
42. J. Heijboer, *Static and Dynamic Properties of the Polymeric Solid State*, R. A. Pethrick and R. W. Richards, Eds., 1982, p. 197.
43. J. D. Ferry, *Viscoelastic Properties of Polymers*, 2nd ed., Wiley, New York, 1969.
44. I. M. Ward, *Mechanical Properties of Solid Polymers*, Wiley, New York, 1971.
45. L. E. Nielsen, *Mechanical Properties of Polymers and Composites*, Dekker, New York, 1974.
46. J. Heijboer, *Int. J. Polym. Mater.*, **6**, 11 (1977).
47. T. Murayama, *Dynamic Mechanical Analysis of Polymeric Material*, Elsevier, Amsterdam, Oxford, New York, 1978.
48. B. E. Read and G. D. Dean, *The Determination of Dynamic Properties of Polymers and Composites*, Wiley, New York, 1978.
49. J. M. G. Cowie, *J. Macromol. Sci. Phys.*, **18**, 569 (1980).
50. T. Murayama, Measurement of Dynamic Mechanical Properties, in Rheology, e.d. G. Astarita, G. Marrucci, and L. Nicolais, Eds., 1980, Vol. 3, p. 397.
51. N. G. McGrum, B. E. Read, and G. Williams, *Anelastic and Dielectric Effects in Polymeric Solids*, Wiley, London, 1967.
52. J. M. Widmaier and G. C. Meyer, *J. Thermal Anal.*, **23**, 193 (1982).
53. R. F. Randel, *Trans. Soc. Rheol.*, **2**, 53 (1958).
54. R. F. Randel and T. L. Smith, *Rubber Chem. Technol.*, **35**, 291 (1962).
55. L. Galperin, *J. Appl. Polym. Sci.*, **11**, 1475 (1967).
56. A. Yim and L. E. St. Pierre, *Polym. Lett.*, **37**, 237 (1967).
57. D. H. Droste and A. T. DiBenedetto, *J. Appl. Polym. Sci.*, **13**, 2149 (1969).
58. Y. S. Lipatov and F. V. Fabulyak, *J. Appl. Polym. Sci.*, **10**, 2131 (1972).
59. K. Disaka and K. Shibayama, *J. Appl. Polym. Sci.*, **22**, 3135 (1978).
60. K. D. Ziegel and A. Romanov, *J. Appl. Polym. Sci.*, **17**, 119 (1973).
61. K. D. Ziegel, *J. Colloid Interface Sci.*, **29**, 72 (1969).
62. A. Yim, R. S. Chahal, and L. E. St. Pierre, *J. Colloid Interface Sci.*, **43**, 583 (1973).
63. R. Stenson, in *Rheology*, G. Astat, G. Marrucci, and L. Nicolais, Eds., 1980, Vol. 3, p. 309.
64. K. Iisaka and K. Shibayama, *J. Appl. Polym. Sci.*, **22**, 1321 (1978).
65. L. E. Nielsen and T. B. Lewis, *J. Polym. Sci.*, **A2**, 7, 1795 (1969).

Received November 15, 1983
Accepted April 19, 1984